AD-A253 637

NTATION PAGE

Form Approved
OMB No. 0704-0188

1. AGENCY USE ONLY (Leave blank)	2. REPORT DATE	3. REPORT TYPE AND DATES COVERED
	3 Feb 1992	Annual Tech 14 Jan 91 - 92

4. TITLE AND SUBTITLE

Spatial Light Modulators with Arbitrary Quantum Well Profiles

5. FUNDING NUMBERS

AFOSR-90-0118 DEF

(2)

6. AUTHOR(S)

George N Maracas
Krishan K Bajaj

7. PERFORMING ORGANIZATION NAME(S) AND ADDRESS(ES)

Arizona State University
College of Engineering and Applied Sciences
Department of Electrical Engineering
Tempe, Arizona 85287-5706

8. PERFORMING ORGANIZATION REPORT NUMBER

DWA_1764

AFOSR-TR- 92 0657

9. SPONSORING / MONITORING AGENCY NAME(S) AND ADDRESS(ES)

AFOSR/NE
Building 410
Bolling AFB , DC 20332-6448

Lamberte

10. SPONSORING / MONITORING AGENCY REPORT NUMBER

3484/A3

11. SUPPLEMENTARY NOTES

12a. DISTRIBUTION / AVAILABILITY STATEMENT

Approved for public release: distribution unlimited

12b. DISTRIBUTION CODE

13. ABSTRACT *(Maximum 200 words)*

This is the year 2 technical report for the University Research Initiative (URI) program "Spatial Light Modulators with Arbitrary Quantum Well Profiles." During the second year of the program we have continued to optimize optical modulator design, growth, and fabrication. A new method for self-consistent solution of Schrödinger and Poisson equations was developed and used to predict modulator active region performance and vertical cavity surface emitting laser device performance. A comprehensive comparison of asymmetric triangular quantum wells (ATQW) using GaAs/AlGaAs, InGaAs/GaAs, and InGaAs/AlGaAs showed InGaAs/AlGaAs quantum wells to have the highest optical efficiency. A MBE compositional grading technique was used to achieve record narrow photoluminescence linewidths for nonrectangular quantum wells. Bragg reflectors for use in Fabry Perot modulators were measured *in-situ* by spectroscopic ellipsometry (SE). Advances were made in the growth and fabrication of p-i-n optical modulators, including the development of via hole etching through the substrate for transmission mode modulators.

A simple variational method for calculating excitonic properties in quantum confined structures with arbitrary potential profiles in the presence of applied electric and magnetic fields were developed and applied to the study of energy levels of hydrogenic impurities. Also a new theory of radiative transition linewidths due to alloy disordering in semiconductor alloys has been presented and applied to AlGaAs and InGaP bulk alloys.

14. SUBJECT TERMS

GaAs (Gallium Arsenide)
InGaAs (Indium Gallium Arsenide)
AlGaAs (Aluminum Gallium Arsenide)
Quantum Well
Spatial Light Modulators
MBE (Molecular Beam Epitaxy)
Excitons

15. NUMBER OF PAGES 42

16. PRICE CODE

17. SECURITY CLASSIFICATION OF REPORT	18. SECURITY CLASSIFICATION OF THIS PAGE	19. SECURITY CLASSIFICATION OF ABSTRACT	20. LIMITATION OF ABSTRACT
UNCLASSIFIED	UNCLASSIFIED	UNCLASSIFIED	UL

Spatial Light Modulators with Arbitrary Quantum Well Profiles

University Research Initiative Program
AFOSR-90-0118 DEF

George N. Maracas
Arizona State University
Electrical Engineering Department
Tempe, AZ

Krishan K. Bajaj
Emory University
Physics Department
Atlanta, GA

TABLE OF CONTENTS

ABSTRACT

This is the year 2 technical report for the University Research Initiative (URI) program "Spatial Light Modulators with Arbitrary Quantum Well Profiles." During the second year of the program we have continued to optimize optical modulator design, growth, and fabrication. A new method for self-consistent solution of Schrödinger and Poisson equations was developed and used to predict modulator active region performance and vertical cavity surface emitting laser device performance. A comprehensive comparison of asymmetric triangular quantum wells (ATQW) using GaAs/AlGaAs, InGaAs/GaAs, and InGaAs/AlGaAs showed InGaAs/AlGaAs quantum wells to have the highest optical efficiency. A MBE compositional grading technique was used to achieve record narrow photoluminescence linewidths for nonrectangular quantum wells. Bragg reflectors for use in Fabry Perot modulators were measured *in-situ* by spectroscopic ellipsometry (SE). Advances were made in the growth and fabrication of p-i-n optical modulators, including the development of via hole etching through the substrate for transmission mode modulators.

A simple variational method for calculating excitonic properties in quantum confined structures with arbitrary potential profiles in the presence of applied electric and magnetic fields were developed and applied to the study of energy levels of hydrogenic impurities. Also a new theory of radiative transition linewidths due to alloy disordering in semiconductor alloys has been presented and applied to AlGaAs and InGaP bulk alloys.

A. Statement of work

The experimental work on this project is performed at Arizona State University under the supervision of Prof. G. N. Maracas. The theoretical effort is under the supervision of Prof. K. K. Bajaj at Emory University.

A.1. Experiment

The progress during the year has been briefly described accordingly. Details can be found in the next section.

* Developed and Implemented Poisson-Schrödinger Solver

A new approach to solving for energy levels and wave functions in a quantum well modulator active region has been developed and implemented. A spectral solution of Schrödinger's equation couples with a self-consistent solution of Poisson's equation has predicted the performance of optical modulators and vertical cavity surface emitting lasers.

* Correlated TEM micrograph with PL data from ATQW

Transmission electron microscopy (TEM) has been used to determine the potential profile in a 286 Å asymmetric triangular quantum well (ATQW). The experimentally determined profile was used as input into the Schrödinger solver. The calculated bound energy levels corresponded to within 1 meV of the bound energy levels measured by optical techniques (both n=1 and n=2 light hole and heavy hole).

* Measured record narrow PL line width for AlGaAs/GaAs ATQW

Photoluminescence spectra of an ATQW has exhibited a record narrow line width (2.1 meV) at 2K . A narrow line width is required for a high on/off ratio of a quantum confined Stark effect (QCSE) modulator. The spectral position of the PL has shown excellent agreement with the theoretical predictions of Gary Sanders.

* Analyzed a variety of quantum well active area designs

The growth and characterization of the active region for quantum well modulators has been studied. Asymmetric coupled double quantum wells (ACDQW), symmetric coupled double quantum wells (SCDQW), ATQW, and rectangular quantum wells (RQW) have been explored for use in high on/off ratio optical modulators. Experimental results from these optical structures agree well with theoretical results.

* Reported first InGaAs/GaAs and ATQW PL

The first coherently strained InGaAs/GaAs ATQWs has been realized. These quantum wells exhibited higher luminescence (factor of five greater) than the equivalent energy rectangular quantum well. This is very encouraging for use as a potential modulator active region.

* Improved PL Intensity for InGaAs ATQW

The PL intensity for InGaAs/GaAs ATMQW structure has been improved by substituting AlGaAs for the barriers. These results are promising for increasing modulator performance.

* Measured first *in situ* AlGaAs/GaAs Bragg reflectors by spectroscopic ellipsometry

In situ spectroscopic ellipsometry has been successfully used to determine the normal incident reflectance of a Bragg reflector. Therefore, the possibility for modulator corrections during the epitaxial layer film growth shows promise for increased modulator yield.

* Compared *ex situ* measurements of AlGaAs/GaAs Bragg reflectors to theoretical results

A test station for the measurement of transmission and reflectance from spatial light modulators has been developed. Measurements of Bragg reflectors have compared favorably with theoretical results. This indicates the functionality of the test station and the high degree of control of the MBE growth process.

* Developed device processing for a variety of spatial light modulators

Refinement of the fabrication process for AlGaAs/GaAs transmission mode, InGaAs/GaAs transmission mode, and AlGaAs/GaAs reflection mode spatial light modulators has progressed well. A jet etching technique has been developed to reliably fabricate optical windows for AlGaAs/GaAs transmission mode modulators.

* Improved InGaAs/GaAs VCSELs device fabrication process

The fabrication of vertical cavity surface emitting lasers (VCSELs) has been refined and improved. An InGaAs/GaAs VCSEL with threshold densities as low as 487 A/cm^2 has been realized.

* Observed light emission from an InGaAlP/InGaP laser structure

The material growth of InGaAlP/InGaP has been explored as a possible means for developing a visible VCSEL. The high quality of the initial material growth of InGaAlP/InGaP at ASU is seen by the emission of light from the edge emitting laser structure.

A.2. Theory

* Developed a simple method for calculating excitonic properties in quantum-confined semiconductor structures with arbitrary potential profiles in the presence of applied fields

A simple but highly efficient, accurate and versatile method to calculate the exciton binding energies, transition energies, oscillator strengths, and absorption coefficients in quantum wells with arbitrary potential profiles in the presence of electric and magnetic fields applied along the growth direction has been developed.

* Developed a new theory of radiative transition linewidths due to alloy disordering in semiconductor alloys

A quantum mechanical formalism for calculating excitonic linewidths due to compositional disorder in semiconductor alloys which eliminates the use of the excitonic volume has recently been developed.

B. Status of the research effort: A substantive statement of significant accomplishments and progress toward achieving the research objectives.

B.1. Experimental realization of nonrectangular quantum well modulators - ASU

B.1.1. Absorption Region Development

B.1.1.1. Theory

1 Development of Poisson-Schrödinger Solver

The active region of a quantum-well optical modulator and a quantum-well laser is defined in terms of the bound state energies and wave functions in the potential well. Determining the bound energies involves solving the coupled Schrödinger and Poisson equations. This requires a self-consistent solution of the eigenvalue/eigenvector problem with a boundary value problem imposed by the Poisson equations. The approach taken here is to represent the Schrödinger equation in Fourier space, which reduces the problem to a linear eigenvalue problem. The next step is to iteratively solve the Schrödinger and Poisson equations.

The approach taken with this work is to begin by solving the general time-independent Schrödinger equation,

$$\left(\frac{-\hbar^2}{2m}\frac{\partial^2}{\partial x^2} + V(x)\right)\Psi(x) = E\,\Psi(x)$$

First, a linear transformation of the Schrödinger equation is done without altering the properties of the equation. A Fourier representation is particularly useful since the differential equation in space is simply an algebraic equation in transform-space.

The wave function ($\Psi(x)$) is represented in terms of its Fourier series; thus it is built from the orthogonal basis, $\exp(jn\pi x/L)$. There is an implicit assumption in using this representation that Ψ is periodic in

the length L. This should not cause any problems since it is the standard boundary condition assumption of "periodic boundaries." In the physical system, this means that little error will be introduced as long as $\Psi(-L/2) \cong \Psi(L/2)$, which is reasonable since the wave function approaches zero at the boundaries of the intrinsic region for bound states. In other approaches to this problem, such as the finite-difference approach, or expansion of the wave function in rigid-box eigenstates, the wave function is forced to zero at these boundaries. The Fourier series representation of $\Psi(x)$ is given by

$$\Psi(x) = \sum_{n=-\infty}^{\infty} c_n \exp(j\frac{n\pi x}{L})$$

which can be directly substituted into the time-independent Schrödinger equation. Next, the equation is multiplied by $\exp(-i\pi kx/L)$ and then integrated over all space. After simplification the Schrödinger equation reduces to

$$\frac{-h^2}{2m} c_k \left(\frac{-\pi k}{L}\right)^2 + \sum_{n=-\infty}^{\infty} c_n d_{n-k} = E\, c_k$$

The Fourier representation of the Schrödinger equation needs to be represented in the form of a discrete Fourier transform (DFT) for numerical computation. By partitioning the potential profile into N divisions, the Fourier series coefficient d_k can be written as

$$d_k = \frac{1}{L} \lim_{N\to\infty} \sum_{n=0}^{N-1} V(x_n) \exp\left(\frac{-j2\pi k x_n}{L}\right)\Delta x$$

using the left-hand integration rule. Thus the DFT coefficients give an approximation of the Fourier series coefficients within a normalization factor.

It is desirable to combine the effects of quantum states and electrical charges or potential when modeling optical modulators or

semiconductor lasers. One way to do this is to solve the Schrödinger equation, and then use the bound states generated to compute a charge-dependent potential function. This potential is then used as the next iteration to solve the Schrödinger equation, and the process is repeated until the potential is constant within some specified tolerance. The equations that describe the Poisson system for the conduction band are

$$V(x) = \Delta Ec(x) - q\phi(x)$$

$$\frac{\partial^2}{\partial x^2}\phi(x) = \frac{-q}{\varepsilon_o}\left[N_D(x) - n(x)\right]$$

$$n(x) = \sum_{k=0}^{m-1} n_k \Psi_k^* \Psi_k$$

and

$$n_k = \frac{m^*}{\pi \hbar^2} \int_{E_k}^{\infty} \frac{1}{1 + \exp[(E-E_F)/kT]}\, dE$$

In the above equations, ΔE_c is the band edge produced by discontinuities due to the hetero-interfaces, $N_D(x)$ is the doping profile, and n(x) is the equivalent carrier density due to the bound states in the well. The wave functions, Ψ_k, are the bound states, E_k are the bound state energies, and there are m bound states; m^* is the effective mass of the electron, and E_F is the quasi-Fermi level for the electrons. A similar set of equations can be written for the heavy-hole and light-hole valence subbands.

The functional blocks of the computer code to solve the Schrödinger and Poisson equations are shown in Figure 1. The Schrödinger equation is solved as a matrix eigenvalue and eigenvector problem in Fourier transform space. The program then solves for the energy bound states and uses the wave functions to determine the band-bending. Iterations between the Schrödinger and Poisson program

yield a self-consistent solution. In Figure 1, the dashed loop indicates the iterations in the main program between the Poisson and Schrödinger programs to arrive at a self-consistent solution.

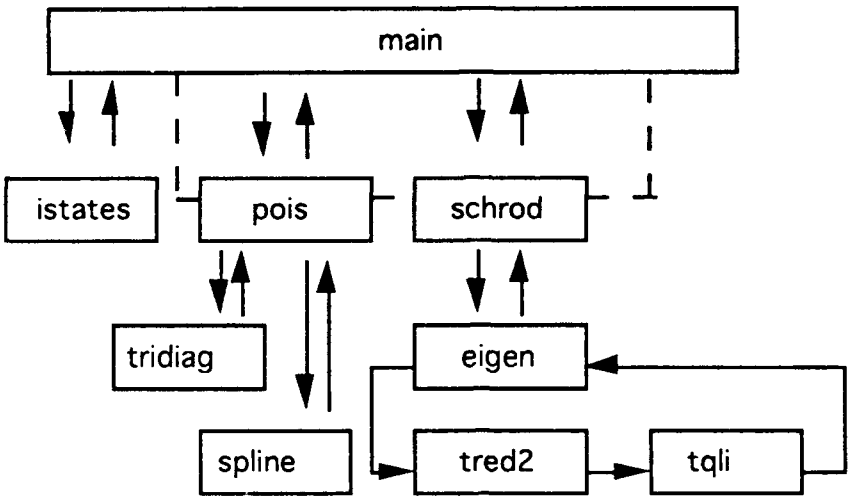

Figure 1 Control flow in Schrödinger-Poisson solution program.

Some of the program's applications are described later in this report. The program is used to calculate the bound energy states from the potential profile obtained from an ATQW transmission electron microscopy (TEM) micrograph and also to predict the performance of vertical cavity surface emitting lasers (VCSELs).

B.1.1.2. Experimental Results

A variety of quantum well structures have been explored for use in the active region of an optical modulator. By simultaneously exploring several active region designs, the optimum active region can be selected for the desired modulator characteristics.

1 Rectangular Quantum Well (RQW) and Asymmetric Triangular Quantum Well (ATQW) Comparison

The ATMQW structure used in this study consists of a 0.25 μm GaAs buffer layer followed by 7 periods of 200 Å/200 Å asymmetric triangular InGaAs multiple quantum well (MQW) and finally a 1000

Å GaAs capping layer. In the asymmetric triangular well the In compositions vary linearly from 0% to 15% across the entire 200 Å width of the well. Since a truly linear compositional grading is difficult to achieve using large thermal mass effusion cells, the variation was approximated using a superlattice compositional grading technique. The period of the superlattice was 25 Å. Within each period, the thickness of the $In_{0.15}Ga_{0.85}As$ layer is made proportional to the required In composition. The resulting structure approximates a continuously graded well in which the average In composition varies linearly with distance.

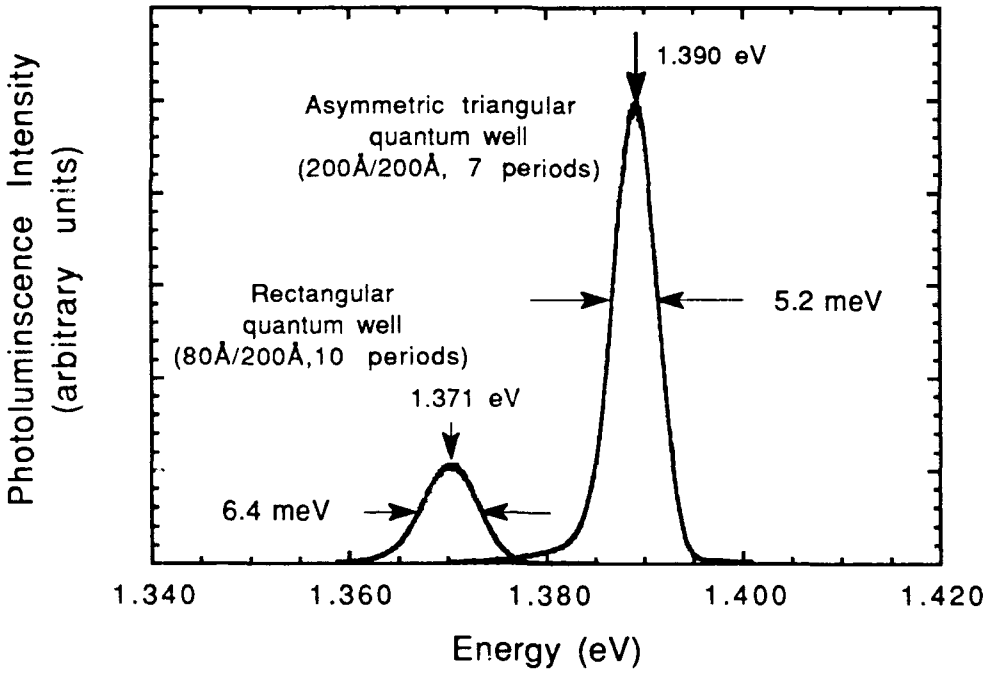

Figure 2 Photoluminescence from InGaAs/GaAs ATMQW and RMQW. For the same active area thickness the ATMQW shows brighter and sharper PL spectra.

For comparison, a 10 period 80 Å / 200 Å InGaAs/GaAs rectangular MQW (RMQW) was grown at 500° C. This structure also consisted of

a 0.25 μm GaAs buffer layer and a 1000 Å GaAs capping layer. All layers were unintentionally doped and grown in succession on the same day.

Note that in both MQW structures the total thickness of the wells and barriers are the same. The total thickness was kept equal since the change in electric field for a given voltage change in a the intrinsic region is directly proportional to the modulator's active region thickness. Therefore, the MQW structures allow a direct comparison of the RMQW and ATQW optical properties. Although the number of rectangular wells is greater than the number of asymmetric wells (ten versus seven) the peak PL intensity for the latter is more than five times greater than the rectangular wells. The PL intensity can be used for comparison since the linewidths are approximately equal. Generally, the integrated intensity is compared. An increase in PL intensity can be attributed to an increase in the carrier collection by the well as a result of compositional grading and/or a decrease in the density of nonradiative recombination centers. Ebner and Arthur[1] observed an increase in PL intensity for InGaAs QWs grown at temperatures above 530°C. This was explained to be due to an increase in the collection of photo-excited carriers in the wells as a result of the internal electric field generated by compositional variation at the top interface caused by In segregation during growth. We believe a similar mechanism is responsible for the enhanced PL intensity observed for the ATMQW structure. In this case the wells are intentionally graded so that a larger number of photo-excited carriers are swept into the wells by the built-in electric field. Thus graded wells can be used to control the collection efficiency of the modulator active region to a higher degree than RQWs. In addition, the use of superlattice type grading has been shown to reduce the density of non-radiative recombination centers.

2 Asymmetric Triangular Quantum Well (ATQW)

1.2.2.1 AlGaAs/GaAs ATQW

A high resolution TEM micrograph of an asymmetric triangular AlGaAs/GaAs quantum well is shown in Figure 3 The discrete layers of AlGaAs and GaAs that were used to approximate the desired compositional grading are shown. On the micrograph, there is an intensity plot which was used to measure the individual layer thicknesses. The potential has been calculated from the TEM micrograph and indicates that the potential is not exactly triangular. The conduction band profile is shown below the TEM micrograph. The valence band potential is not shown, but is calculated using a fixed band offset. The measured energy band diagram was then input into the Schrödinger solver. The numbers to the left and right of the well denote the measured and calculated optical transition energies respectively. The agreement between theory and the measured potential is approximately 1 meV for the lowest three states (n=1 lh & hh and n=2 lh & hh). Measured well energies were obtained from photocurrent experiments.

The photoluminescence from an AlGaAs/GaAs asymmetric multiple quantum well is shown in Figure 4. The structure is composed of a one micron buffer layer of AlGaAs. Next , the active region is composed of eleven 675 Å asymmetric AlGaAs/GaAs triangular quantum wells with 80 Å AlGaAs spacers. Finally a 0.5 μm AlGaAs cap layer was grown. The energy of the 2 K photoluminescence peak corresponds to the calculated energy (See inset in Figure 4) using software developed by Gary Sanders. A linear compositional profile was used. This FWHM is the narrowest reported for an AlGaAs/GaAs ATMQW. The narrow line width is required to increase the on/off ratio of the quantum confined Stark effect modulator. These results indicate that the compositional grading has been developed to a degree which allows comparison with theories using simple algebraic potential functions as well as superlattice profiles.

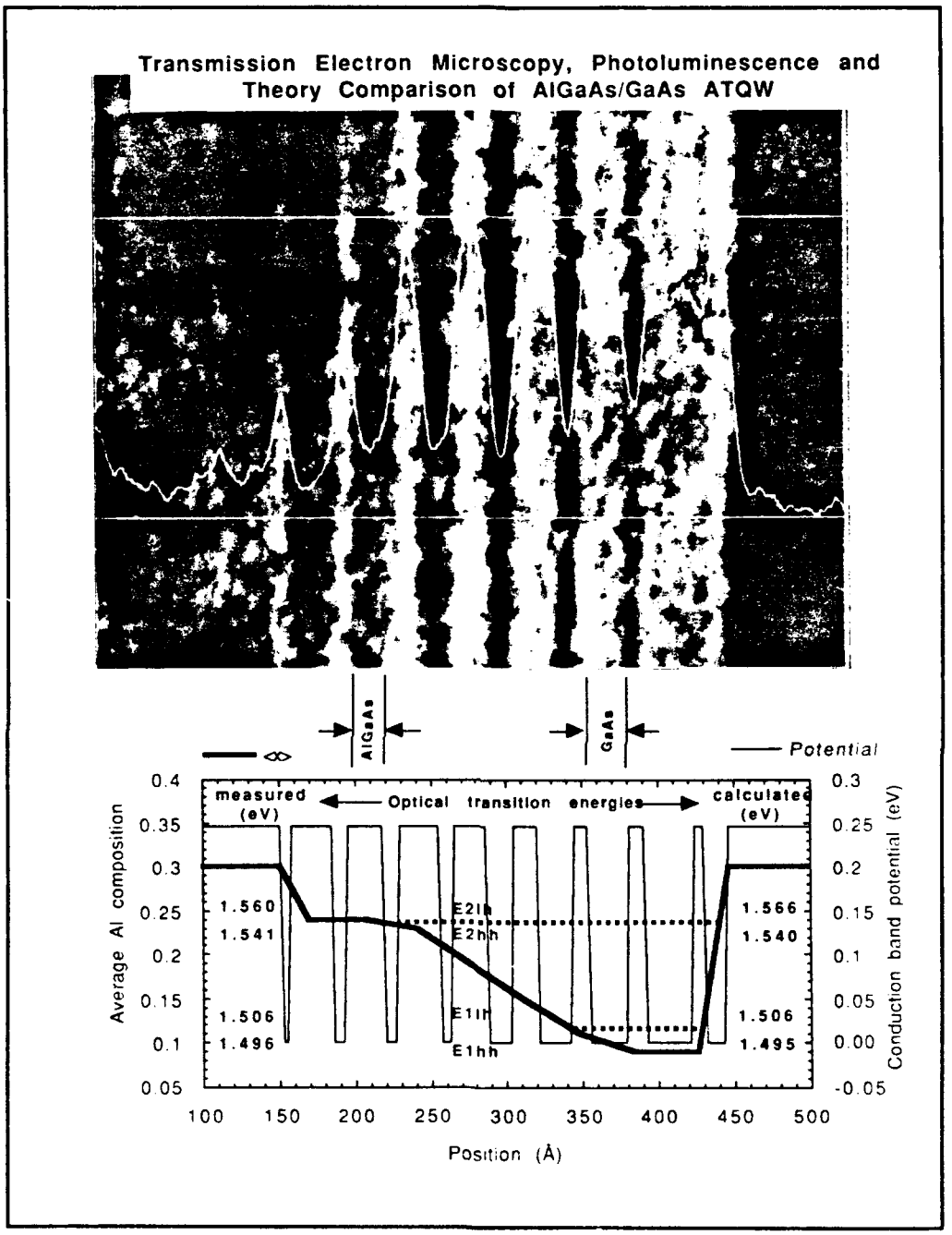

Figure 3 Transmission electron microscopy is used to determine the potential profile of the AlGaAs ATQW. Then the Schrödinger FFT program is used to calculate the photoluminescence transition energies.

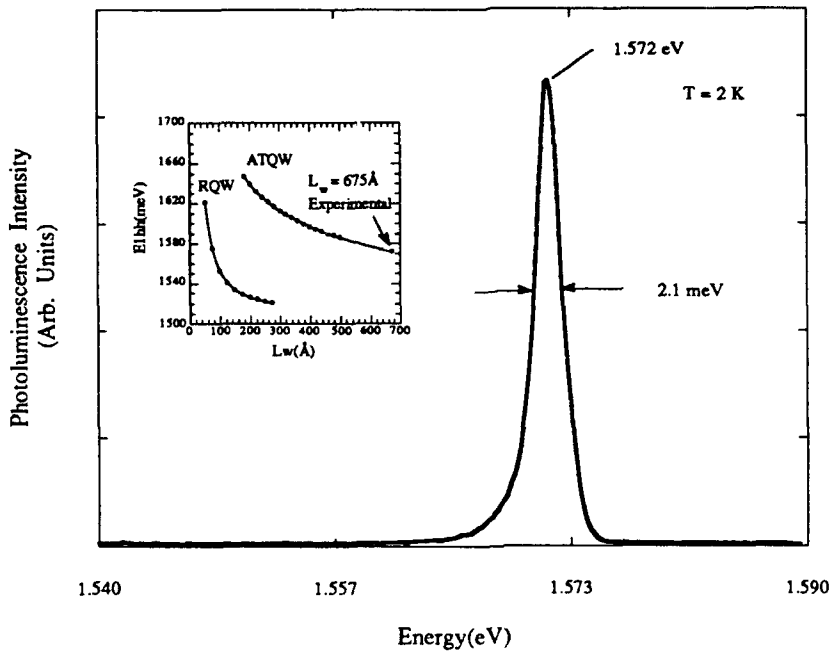

Figure 4 Photoluminescence from a 675 Å an AlGaAs/GaAs asymmetric triangular quantum well. Record narrow FWHM for an AlGaAs/GaAs ATQW.

1.2.2.2 InGaAs/GaAs and InGaAs/AlGaAs ATQW

The photoluminescence intensity for InGaAs/GaAs and InGaAs/AlGaAs asymmetric triangular quantum wells is shown in Figure 5. The InGaAs/AlGaAs MQWs exhibit a dominant excitonic peak due to the recombination of the n=1 electron to heavy hole transition. In this type of quantum well structure the band gap difference between the barrier and well material is much larger than the band gap difference for the InGaAs/GaAs QW. As a result, the conduction band discontinuity, ΔE_c, is larger which results in a deeper well and an increase in the confinement energy of the wells. As shown in Figure 5, the deeper well exhibits a more intense

excitonic peak which is encouraging for producing high on/off ratio optical modulators.

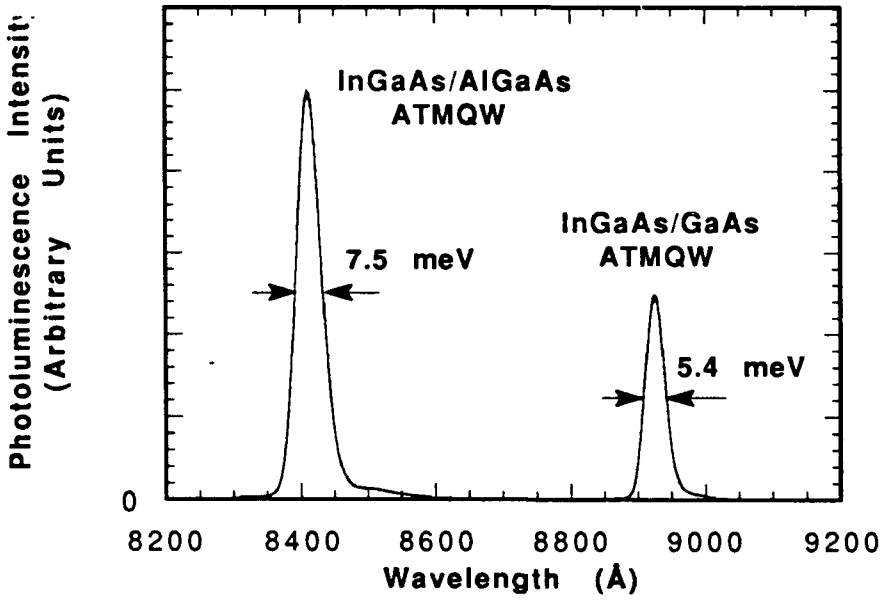

Figure 5 Photoluminescence spectra taken for a 7-period 200 Å/200 Å $In_{0.15}Ga_{0.85}As/Al_{0.30}Ga_{0.70}As$ ATMWQ and a 7-period 200 Å/200 Å InGaAs/GaAs ATMQW.

A series of InGaAs asymmetric triangular quantum wells has recently been grown . These wells were grown at a temperature of 500° C as measured by an optical pyrometer. The GaAs growth rate was 0.8 μm/hr and the As:Ga flux ratio was 2.5:1. which was measured with RHEED intensity oscillations. The InGaAs was designed to be 10% In and the triangular wells were approximated with a superlattice grading technique. The photoluminescence from these structures indicates a record narrow FWHM. Further characterization and analysis is being done on these structures. For the first time sub meV linewidths have been obtained in compositionally graded wells.

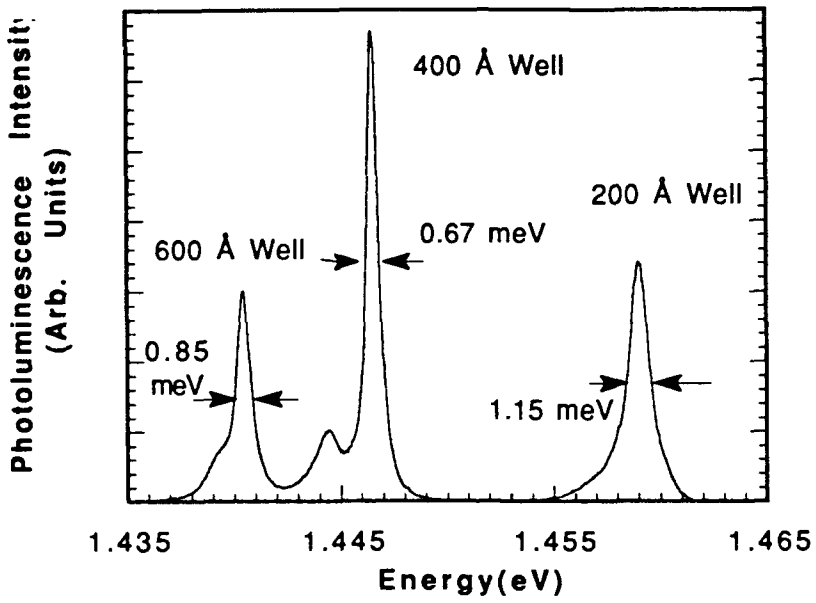

Figure 6 Photoluminescence intensity for InGaAs ATQWs.

3 Coupled Double Quantum Wells (CDQW)

An alternate approach for an optical modulator is to use coupled double quantum wells (CDQW). Two type of CDQWs have been explored, the asymmetric and the symmetric. Initially, a one micron buffer layer of AlGaAs was grown, followed by 33 coupled wells separated by 80 Å of AlGaAs. The profiles for the active regions are shown in the insets of Figure 7. Finally a 0.5 μm AlGaAs cap layer was grown. The double peak in the symmetric CDQW is due to a monolayer change in the well width of the top layers of the multiple quantum well structure. The arrows denote the calculated transition energies. The 2 K photoluminescence line width is a respectable 2. meV. These calibration runs have allowed for the design of optical modulators using CDQWs. The optical modulators are currently being fabricated and characterized.

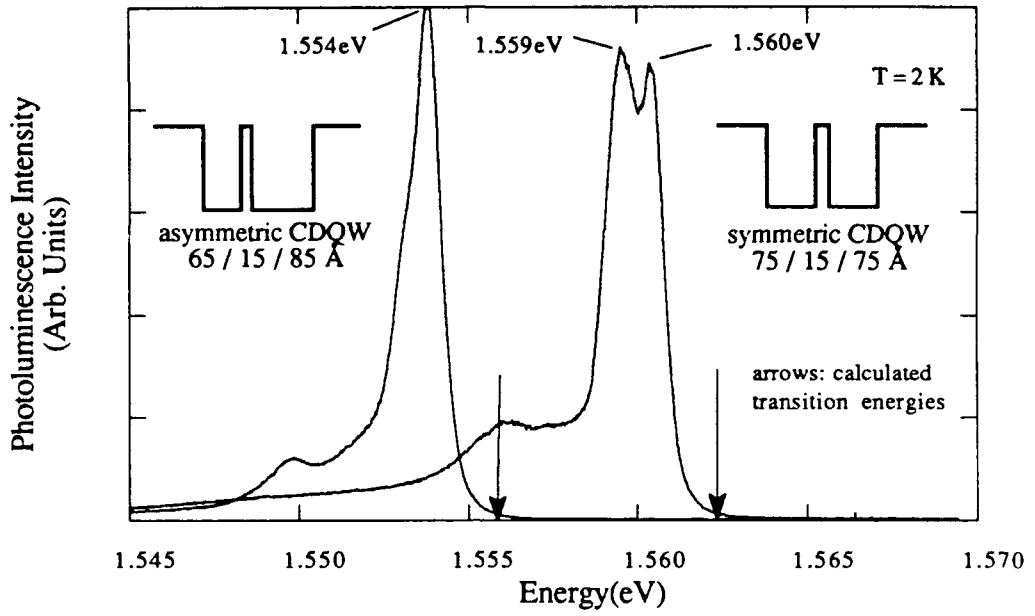

Figure 7 Photoluminescence from symmetric CDQWs and asymmetric CDQWs.

B.1.2. Distributed Bragg Reflectors (DBR)

B.1.2.1. In situ Measurements of AlGaAs/GaAs Bragg Reflectors by Spectroscopic Ellipsometry

The first *in situ* measurements of AlGaAs/GaAs Bragg reflectors by spectroscopic ellipsometry has been performed. An AlGaAs/AlAs Bragg reflector was grown which is composed of 10 periods of $Al_{0.3}Ga_{0.7}As$/AlAs. The structure was then cooled to near room temperature and spectroscopic measurements were taken between 2500 Å and 1 μm at a fixed angle of incidence of approximately 75°. The ellipsometric parameters Ψ and Δ were measured and modeled to determine the true AlGaAs and AlAs thickness. The measured thicknesses were then used to calculate the normal incident reflectance. Subsequently, *ex situ* measurements of the Bragg reflector were taken and the values of Ψ and Δ were essentially identical to the *in situ* measurements except for differences in the

short wavelength region. The *ex situ* differences in Ψ and Δ are consistent with an oxide layer formed on the surface of the Bragg reflector. Therefore, the *ex situ* ellipsometric measurements are further confirmation of the *in situ* measurements.

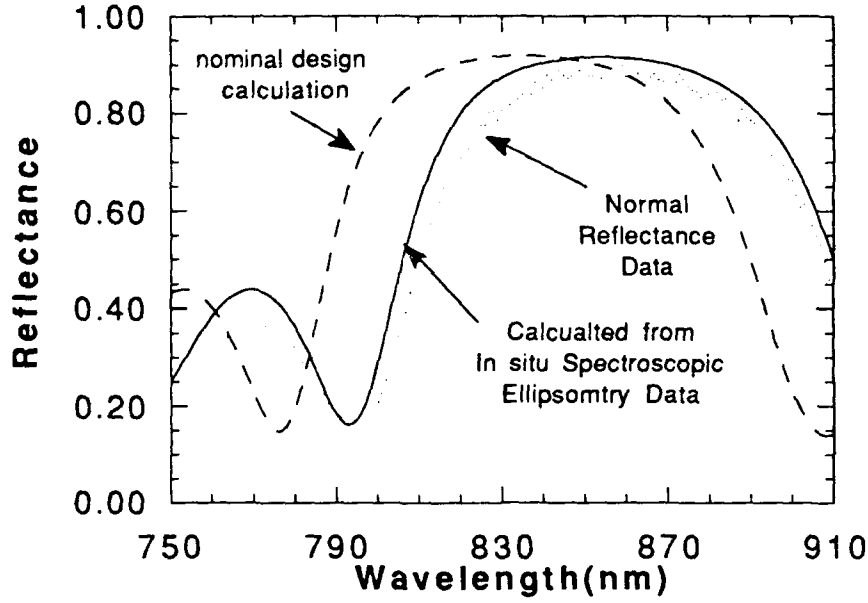

Figure 8 In situ spectroscopic ellipsometric evaluation of AlGaAs/GaAs Bragg reflector.

The thickness parameters extracted from the *in situ* measurements for the AlGaAs(749 Å)/AlAs(603 Å) were then used to compute the normal incidence reflectance which is shown in Figure 8. The design thicknesses for the AlGaAs and AlAs were 700 Å and 614 Å respectively. As shown in Figure 8 the thickness deviations caused the normal incident reflectance curve to shift toward higher wavelengths. The normal incident reflectance was measured *ex situ* with a Ti-Al_2O_3 laser from 7500 Å to 9100 Å. The measured data compares very well with the normal incident reflectance data which was computed from the *in situ* ellipsometric data. Therefore, by measuring the Bragg reflection *in situ* , corrections could possibly be made to cavity dimensions during the growth of the optical

modulator or vertical cavity surface emitting laser. Such capability would increase the device yield. The *in situ* measurements also aid in the device analysis. Some work still needs to be done in obtaining high temperature optical constants of AlGaAs.

B.1.3. Processing Steps for Spatial Light Modulators

Processing of optical modulators has taken place in three areas: AlGaAs/GaAs transmission modulators, InGaAs/GaAs transmission modulators, and AlGaAs/GaAs reflection modulators. Each type of modulator requires special processing steps because of the transmission properties of the substrate. In the case of AlGaAs/GaAs modulators, the optical transmission wavelength takes place above the band gap of GaAs. Therefore, the GaAs substrate must be removed or thinned to reduce absorption in the substrate. The InGaAs/GaAs transmission modulator benefits from the fact that the transmission energy can be tuned to less than the band gap of GaAs and therefore, does not require substrate removal. Lastly, neither InGaAs/GaAs or AlGaAs/GaAs reflection modulators require the removal of the substrate.

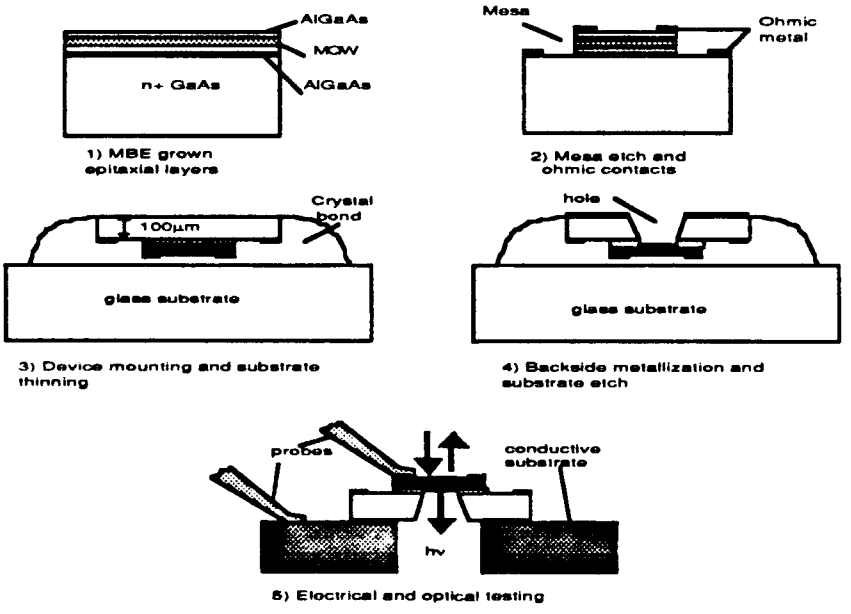

Figure 9 AlGaAs/GaAs optical modulator fabrication steps.

AlGaAs/GaAs pin-transmission modulators are composed of a multiple quantum well inserted between a p-type and n-type AlGaAs layer. The structures are grown on GaAs substrates. The first processing step is to define mesa diodes using a wet etch. Ohmic contacts are then made to the p-type AlGaAs top surface through standard metal lift-off techniques. Next, the GaAs substrate is then lapped to approximately 100 μm. A metal pattern is then defined on the backside of the substrate which acts as both an ohmic contact

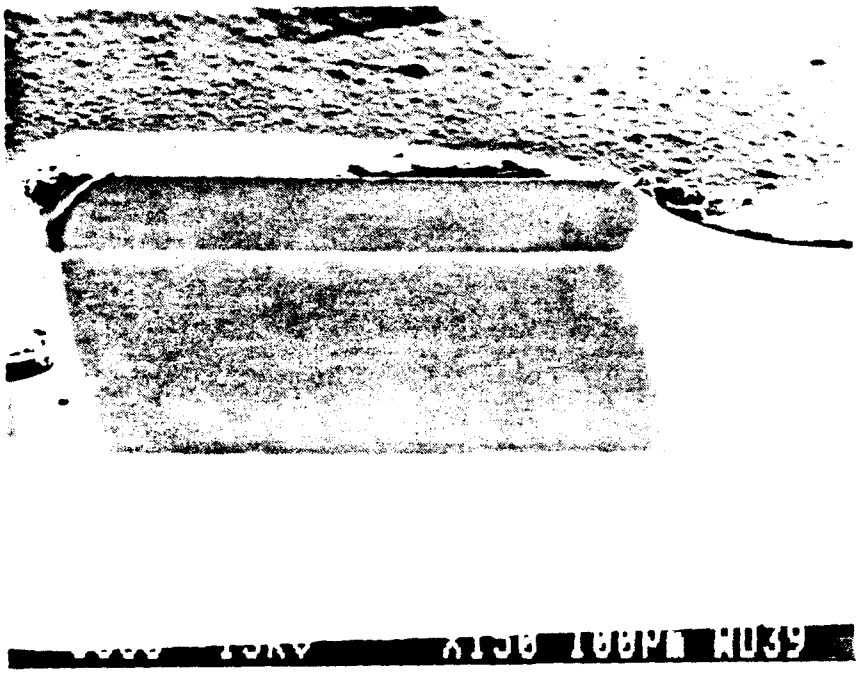

Figure 10 SEM photograph of an AlGaAs/GaAs pin modulator seen through an optical window etched through the substrate.

and an etch mask. A hole is etched through the backside of the substrate, stopping within the n-type AlGaAs epitaxial layer. The back side etch is accomplished with a modified jet etching instrument from South Bay Technology. The jet etcher provides a stream of $NH_4OH:H_2O_2$ directed at the backside of the wafer while monitoring the transmission through the wafer. Once the instrument detects that the substrate has been removed, the etch is terminated.

The etch rate of GaAs in $NH_4OH:H_2O_2$ is increased from 6 μm/hr in magnetically stirred beaker to 80 μm/hr with the jet etcher which results in a significant reduction of processing time. The selectivity between AlGaAs and GaAs etch rates is increased from 10:1 to 16:1 which allows for better control in stopping the etch at the beginning of the AlGaAs layer

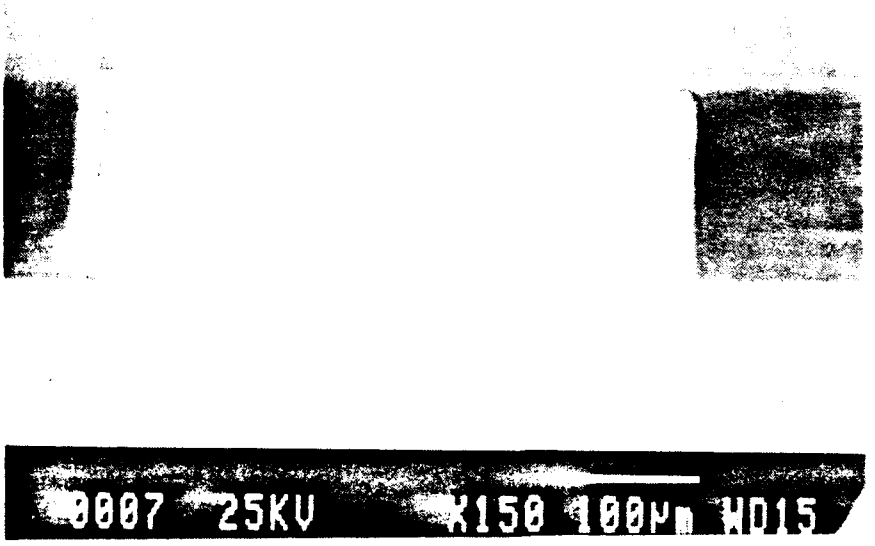

Figure 11 Cathodoluminescence from a 2.4 μm p-i-n optical modulator as seen through an optical window

An example of an AlGaAs/GaAs pin modulator with an optical window jet etched through the back side of the substrate is shown in Figure 10. The substrate is completely etched away and the epitaxial layer is exposed through the etched optical window. The back side of the GaAs substrate has been coated with carbon dag for SEM viewing purposes. The actual p-i-n thickness is approximately 2.4 μm thick and is supported on a GaAs slab for support during cleaving. The high degree of thickness uniformity and material quality can be seen in the room temperature cathodoluminescence from the p-i-n structure (Figure 11).

The transmission mode InGaAs/GaAs modulator fabrication proceeds in much the same way as the AlGaAs/GaAs modulator except the substrate thinning and etching is not required because the operating wavelength of the InGaAs/GaAs is not absorbed by the GaAs substrate. Likewise, the reflection mode devices only require simple processing since they are only optically addressed from the surface. For both the InGaAs/GaAs transmission modulators and the reflection modulators, the processing simply consists of defining mesa diodes through a wet chemical etch and then contacting the diodes through standard metalization techniques.

B.1.4. Spatial Light Modulator Performance

B.1.4.1. InGaAs/GaAs Asymmetric Triangular Quantum Well

A p-i-n modulator structure was grown with an InGaAs/GaAs ATMQW active region. Preliminary results from the photoluminescence (Figure 12) of this structure show very narrow (1.1 meV) FWHM from the InGaAs/GaAs ATMQW region indicating a high material quality with sharp, abrupt interfaces. Fabrication and testing of this device is currently in progress.

B.1.5. Vertical Cavity Surface Emitting Laser (VCSEL)

A variety of optical architectures and signal processing applications could be realized with a two-dimensional array of vertical cavity surface emitting lasers (VCSELs) coupled to a two-dimensional array of spatial light modulators.

One area of interest is in the growth of InGaAs VCSELs which are of particular interest because of their emission at energies below the band gap of GaAs. This allows the coupling of AlGaAs/GaAs transmission modulators without removal of the modulators' substrate which simplifies the modulator fabrication.

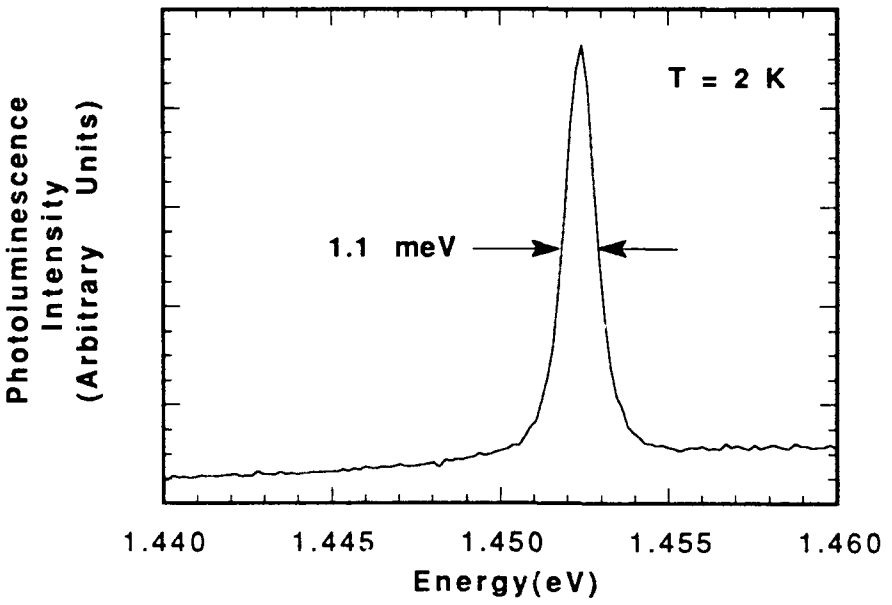

Figure 12 Photoluminescence from an InGaAs/GaAs p-i-n optical modulator.

The design of an InGaAs/GaAs VCSEL has been studied using the Schrödinger-Poisson solver. Current injection has also been included to simulate laser devices. The computer simulation allows optimization of the device design prior to material growth and fabrication. The Schrödinger-Poisson solver was used to calculate gain profiles as a function of wavelength and doping concentrations. The laser threshold current density was also computed for a variety of structures.

Development of a fabrication process for VCSELs has resulted in the master's thesis of J. P. D. Suryanata as well as collaborations with Motorola in Tempe, Arizona. The results of this work have achieved a record (at the time of fabrication) low threshold current density for a VCSEL of 487 A/cm^2 in continuous wave, room temperature operation. The low threshold current is attributed to the

optimization of the compositional grading and the high optical efficiency of the InGaAs grown at ASU.

Another area of interest has been for the development of a visible VCSEL. The band gap of GaAs/AlGaAs is not large enough to provide room temperature laser emission in the yellow portion of the spectrum. Therefore, quaternary/ternary (GaAl)InP/InGaP that is lattice matched to GaAs has been chosen for the development of the visible semiconductor laser.

An initial step toward the VCSEL has been the growth of an edge emitting laser for the purpose of studying the molecular beam epitaxial growth and the characterization (both optical and electrical) of InGaAlP/InGaP material. The initial edge emitting laser was grown in a VG V80H gas source MBE (GSMBE). Prior to growth of the InGaAlP laser structure, the fluxes for Ga and Al were calibrated from RHEED intensity oscillations of GaAs and AlAs. The In flux was calibrated from RHEED intensity oscillations of InP. The InGaP and InGaAlP were grown at substrate temperatures of 480° C and 510° C respectively. A pn-junction was formed using Si and Be for the p-type and n-type dopants, respectively. This laser structure had a specular surface. The DH laser structure showed spontaneous light emission at room temperature under pulsed excitation.

These results are very encouraging considering that they are initial growths of InGaP and InGaAlP for the research group. Further optimization of the material growth, device design, and fabrication is under way. Many of the fabrication process development for the InGaAs/GaAs/AlGaAs VCSELs will be directly applicable to the InGaAlP/InGaP VCSEL.

B.2. Theoretical treatment of nonrectangular well modulators- Emory University

B.2.1. A SIMPLE METHOD FOR CALCULATING EXCITONIC PROPERTIES IN QUANTUM-CONFINED SEMICONDUCTOR STRUCTURES WITH ARBITRARY POTENTIAL PROFILES IN THE PRESENCE OF APPLIED FIELDS

B.2.1.1. Introduction

We have developed a simple but highly efficient, accurate and versatile method to calculate the exciton binding energies, transition energies, oscillator strengths and absorption coefficients in quantum wells with arbitrary potential profiles in the presence of electric and magnetic fields applied along the growth direction [2,3]. We have studied the excitonic properties in square, parabolic, and asymmetrical triangular quantum-well structures in the presence of electric and magnetic fields.

This method can also be applied to describe the electronic states of a donor in a quantum well with an arbitrary potential profile in the presence of both the electric and magnetic fields applied along the growth direction. We have calculated the values of the binding energy of the ground state of a donor located in a coupled double quantum well structure as a function of its position, the well width, and electric and magnetic fields.

B.2.1.2. Formulation

We have developed a powerful variational formalism in which the analytical form of the trial wavefunction is approximated using a variational function for the electron and hole correlated motion along the growth direction in a highly confined quantum well structure. This variational function is then determined approximately through evaluating a double integral. Such a simple procedure saves much valuable computation time in obtaining many important properties of excitons in quantum well structures. We have calculated the

values of the binding energies, transition energies and oscillator strengths of both the heavy-hole and the light-hole excitons in square and asymmetrical triangular quantum-well structures in the presence of an electric field applied parallel to the direction of growth. The results thus obtained are in good agreement with those of other calculations. We have also applied this formalism to study the excitonic properties in quantum confined structures with arbitrary potential profiles in the presence of a magnetic field applied parallel to the growth direction using an appropriate form of the trial wavefunction. And finally, we have extended our formalism to the case where both the electric field and the magnetic field are applied simultaneously. The main advantage of our formalism lies in the fact that we need to determine only one variational parameter for the case where both the electric and the magnetic fields are present simultaneously. Therefore, exciton wavefunctions, binding energies and oscillator strengths are much easier to obtain than optimizing a multidimensional integral equation of several variational parameters in the conventional variational approaches.

We have also adapted our formalism to calculate the energy levels of a hydrogenic impurity in a coupled double quantum well structure in the presence of electric and magnetic fields by letting the hole mass go to infinity and the hole subband wavefunction to a delta function.

B.2.1.3. Excitonic Properties in an Electric Field

We have calculated the binding energies and oscillator strengths of both the heavy-hole and the light-hole excitons in a $GaAs/Al_{0.3}Ga_{0.7}As$ square quantum well as a function of well width and applied field strengths. The exciton binding energy decreases as field strengths increases. Although our calculated exciton binding energies are almost the same as those of Sanders and Bajaj[4] over a wide range of well widths and electric fields, our oscillator strengths are about 40 % higher than theirs. However, our values of the oscillator strength are closer to those of Bauer and Ando[5].Also our oscillator strength follow a correct trend as a function of well width and applied electric field strength.

The asymmetrical triangular quantum well structures are expected to have higher contrast ratios than those of square well and parabolic well structures[4]. The exciton binding energy and oscillator strength versus well width for heavy-hole excitons in the asymmetrical triangular quantum wells at a few applied electric field strengths are shown in figure 1. When the applied field is large enough, the confining potential for either the electron or the hole disappears in the asymmetrical triangular quantum well, thus, the bound state in the quantum well ceases to exist. As shown in Fig. 1(a), the exciton binding energy drops rapidly near Lw = 400 Å at F = 40 kV/cm. This indicates a drop in the hole potential of 0.16 eV that is larger than the confining potential barrier E_V = 0.151 eV. The two-dimensional enhancement of the optical absorption can be switched on and off by a small change in the applied electric field under a specific biased condition. The largest field-induced change in the oscillator strength can be obtained under the biased condition where the heavy-hole confining potential vanishes due to the applied electric field, as one can observe from Fig. 1(b) at F = 40 kV/cm and F = 60 kV/cm for the well widths of 400 and 250 Å, respectively. Thus, in these operating regions one can expect an excellent performance of the modulators.

B.2.1.4. Excitonic Properties in a Magnetic Field

We have used our formalism to calculate the binding energies and the oscillator strengths of the both the heavy-hole and the light-hole excitons in square, parabolic and asymmetrical triangular quantum well structures in the presence of a magnetic field. The exciton binding energies obtained using our approach in the case of square wells agree very well with previous calculations [6,7]. For a given well size our calculated binding energies and oscillator strengths increase as the magnetic field increases, due to larger in-plane confinement of the electrons and holes. At high magnetic fields, we have a quasi-zero-dimensional exciton and the oscillator strength becomes very large.

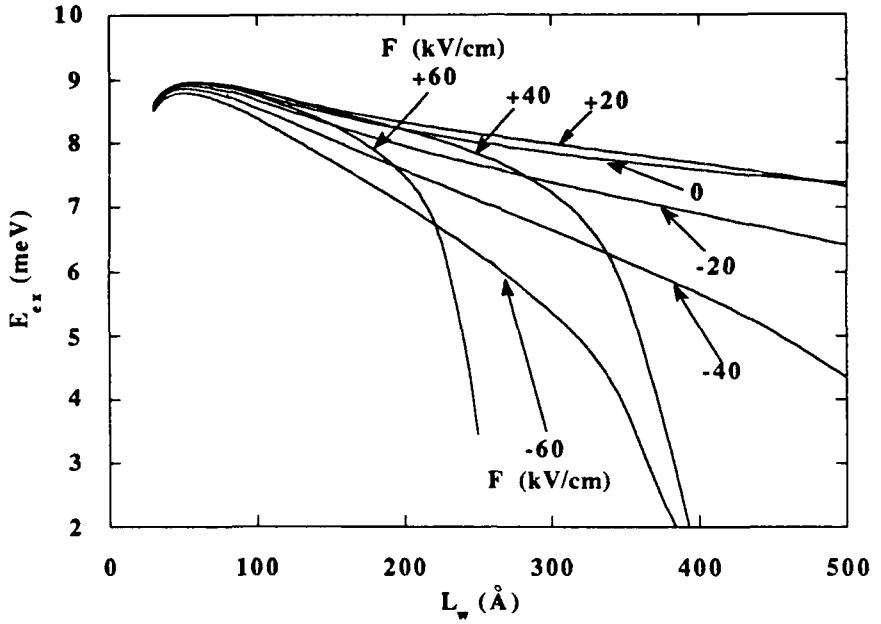

(a)

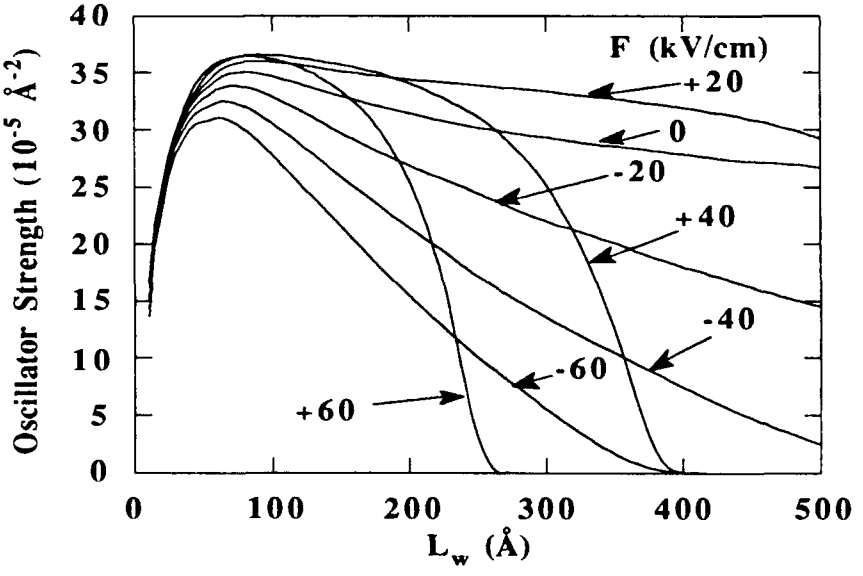

(b)

Fig. 1 Variation of the (a) the heavy-hole exciton binding energy (E_{ex}), (b) oscillator strength as a function of well width (L_w) in a GaAs-$A_{0.3}Ga_{0.7}A$s asymmetric triangular well for several values of the electric field (F).

In Fig. 2, we show the variations of the heavy-hole exciton binding energies and oscillator strengths in an asymmetrical triangular quantum well as a function of well width for several values of the magnetic field. The exciton binding energies and the oscillator strengths follow the same trends as those in the square quantum wells. However, they are less sensitive to the well width variations compared to those in the square wells.

B.2.1.5. Excitonic Properties in both an Electric and a Magnetic Field

In Fig. 3 we show the variations of the heavy-hole exciton binding energies and oscillator strengths as a function of well width in a square-quantum well in the presence of a few typical applied electric and magnetic field strengths [8]. The binding energies and oscillator strengths are grouped by the magnetic field strengths. For the sake of clarity of display we shift the horizontal axes (the quantum well widths) for the curves with Bz=50 kG, 100 kG, 150 kG, and 200 kG by 100 Å, 200 Å, 300 Å, and 400 Å, respectively.

The exciton binding energies and the oscillator strengths increase with the increase in magnetic field, but decrease with the increase in the electric field as expected. In a given magnetic field and for narrow wells, the exciton binding energies and oscillator strengths are relatively insensitive to the applied electric field because the electron and the hole cannot be pulled far apart from each other due to the strong confining potentials. However, we can obtain significant electric field induced changes in these quantities for relatively large well widths (Lw $\geq$ 100 Å) due to large electric field induced electron and hole separations in wide quantum wells. The electric field induced changes in the exciton binding energies and oscillator strengths at any given well width increase as the applied magnetic field strength increases. For example, the electric field induced changes in oscillator strength from F=0 to 100 kV/cm in the 100 Å quantum well are 14 (10^{-5} Å^{-2}) and 27 (10^{-5} Å^{-2}) for Bz=0 and B_z=200 kG, respectively. In a narrow well, in the presence of a strong magnetic field, the excitonic behavior in quantum wells resembles to that in quantum dots.

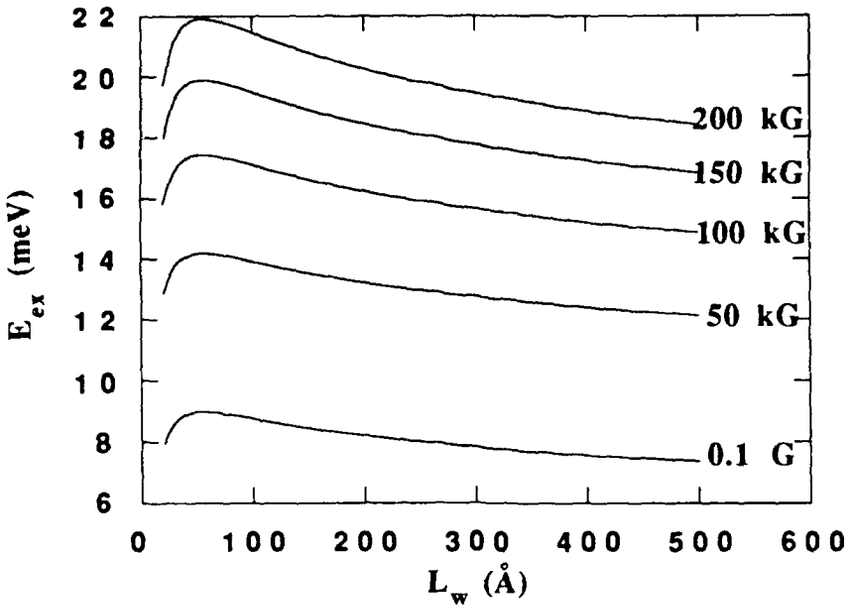

(a)

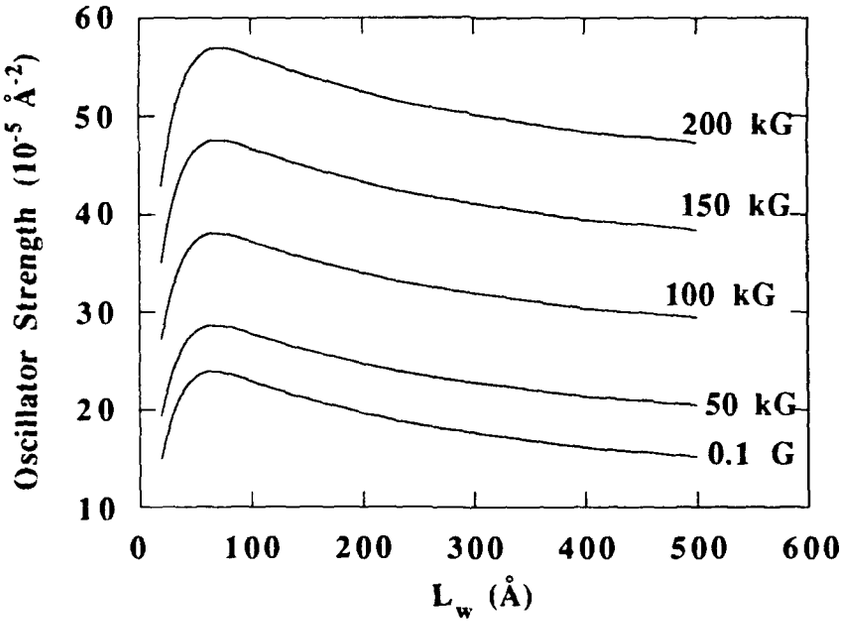

(b)

Fig. 2 Variations of the (a) the heavy-hole exciton binding energy (E_{ex}), and (b) oscillator strength as a function of well width (L_W) in a GaAs-$A_{0.3}Ga_{0.7}As$ asymmetric triangular well for several values of the magnetic field strength.

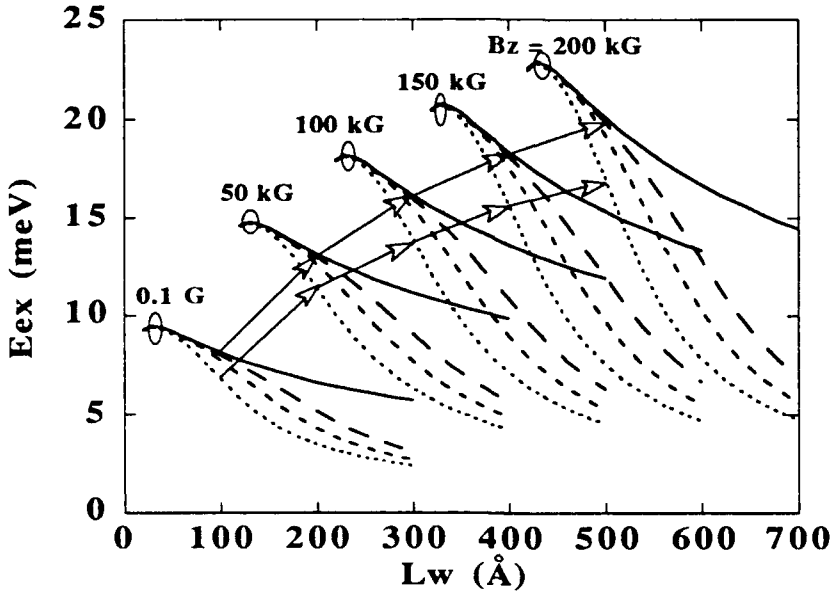

Fig. 3 Variation of the heavy-hole exciton binding energy (E_{ex}) as a function of well width (L_w) in a GaAs-$A_{0.3}Ga_{0.7}As$ square well for several values of the magnetic and electric field strengths. The quantum well width axis are shifted by 0 Å, 100 Å, 200 Å, 300 Å, and 400 Å for the magnetic field strengths of 0.1 G, 50 kG, 100 kG, 150 kG, and 200 kG, respectively. The solid lines are for the electric field strength F = 0; the long dashed lines are for F=20 kV/cm; the dashed lines are for F=40 kV/cm; the dotted lines are for F=100 kV/cm.

B.2.1.6. Confined Donor States in a Coupled Double Quantum Well

We have adapted our formalism to calculate the energy levels of a hydrogenic impurity in an arbitrary potential well in the presence of electric and magnetic fields.

In Fig. 4, we show the variation of the binding energy of the ground state of a hydrogenic donor as a function of the electric field, at zero magnetic field, in a asymmetrically coupled quantum well (ACDQW) structure with well widths of 50 Å and 20 Å, and the barrier ($Al_{0.3}Ga_{0.3}As$) width of 25 Å. We consider the donor at the center of the wide well. In a double quantum well structure

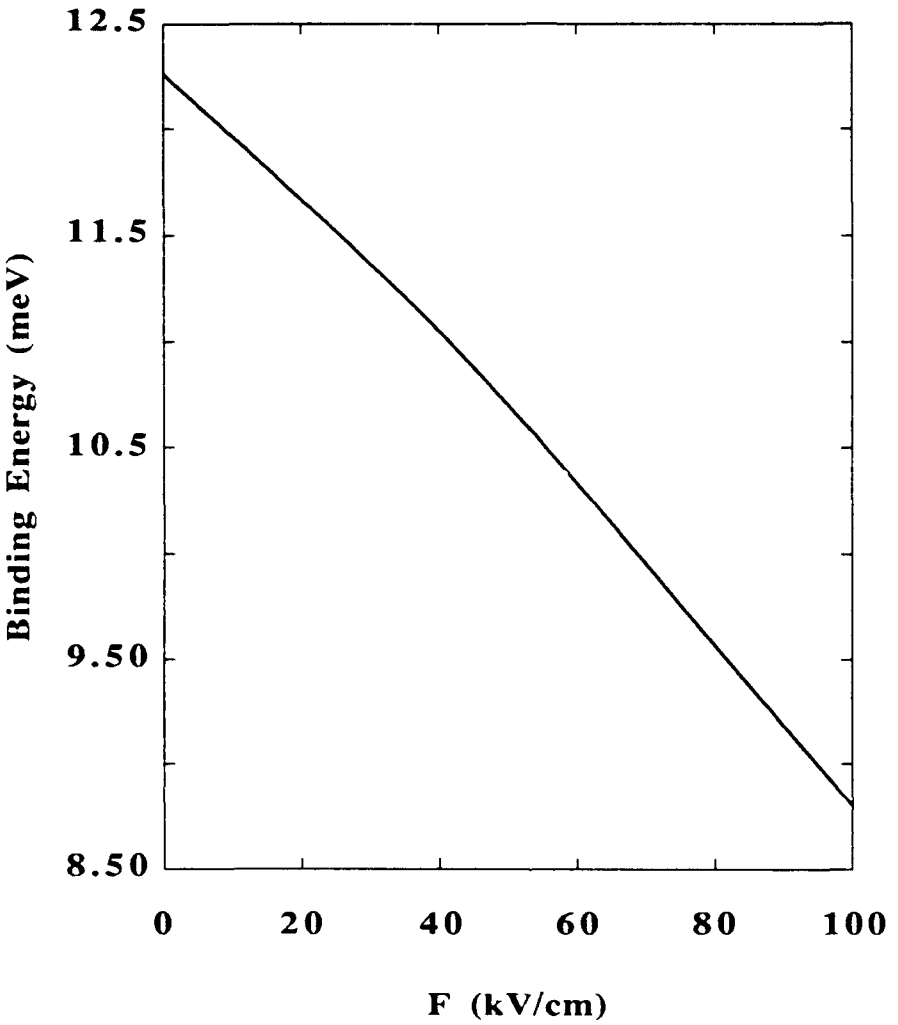

Fig. 4 variation of the binding energy of the ground state of a hydrogenic donor as a function of the electric field in a asymmetric double quantum well with well widths of 50 Å and 20 Å, and the barrier width (GaAs-$A_{0.3}Ga_{0.7}As$) of 25 Å. The donor is located at the center of the wider well.

consisting of a wide well and a narrow well separated by a thin barrier, the ground state electron wave function is concentrated in the wide well in the absence of an electric field, and thus the binding energy of the donor in the wide well is higher in the absence of the applied electric field. As the electric field is increased, the electron is pulled towards the narrow well, and can tunnel across the thin barrier, away from the donor ion in the

wide well. The binding energy of the donor in the system therefore decreases. Although a similar behavior in an electric field was also found for donors distributed in a single quantum well, the rate of change in the binding energy is significantly higher in an ACDQW, due to the easy redistribution of the electron wave function across a thin barrier in an electric field. Similar behavior of the donor binding energy with electric field is also found in the presence of a magnetic field applied parallel to the direction of growth.

B.2.2. A NEW THEORY OF RADIATIVE TRANSITION LINEWIDTHS DUE TO ALLOY DISORDERING IN SEMICONDUCTOR ALLOYS

B.2.2.1. Introduction

The excitonic transitions in semiconductor alloys are generally broader than those observed in their components. This broadening is attributed to the compositional disorder present in the alloys. Early calculations of the excitonic linewidths in random alloys treat an exciton as a classical system with a finite volume, and the alloy composition fluctuation in this exciton volume is obtained using the method of Lifshitz [9,10]. We have recently developed a quantum mechanical formalism for calculating excitonic linewidths due to compositional disorder in semiconductor alloys which eliminates the use of the exciton volume. Using a quantum mechanical description for the excitonic system, the mean deviation of the excitonic transition energy associated with the statistical potential fluctuations is calculated using a first order perturbation theory. We then apply this theory to calculate the linewidth for the ground state excitonic transition as a function of the average alloy composition. Specifically, the excitonic linewidth in $Al_xGa_{1-x}As$ alloy as a function of Al composition x is calculated and compared with an earlier model and with available low-temperature photoluminescence data.

Application of a magnetic field modifies the exciton wavefunctions in semiconductor alloys, thus, providing another way to probe the sample. For an exciton in a magnetic field, the choices of

exciton volume to be used are not obvious, because the exciton wavefunctions are not spherically symmetric. We have used our formalism to study the variation of the excitonic linewidth as a function of the magnetic field due to alloy disordering and specifically apply it to the $Al_xGa_{1-x}As$ and $In_xGa_{1-x}P$ alloys.

B.2.2.2. Alloy Broadening in $Al_xGa_{1-x}As$

In Fig. 5, full width at half maximum (σ) of an excitonic transition is plotted as a function of Al composition. The solid curve is obtained with our approach and the dashed curve is based on the work of Singh and Bajaj[9]. While σ increases with the Al composition in both models as expected, their calculation overestimates the effect of

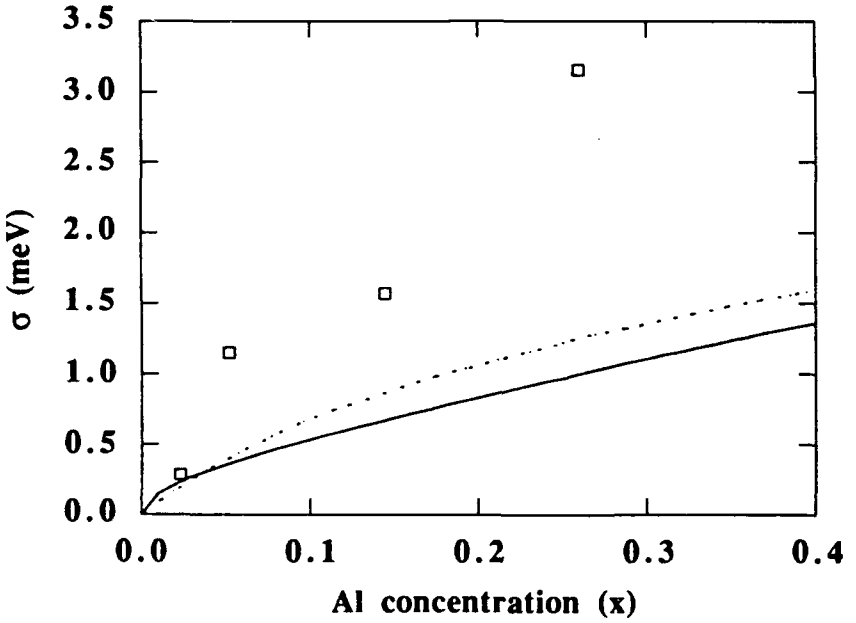

Fig. 5 Variation of the full-width at half-maximum (σ) of the excitonic transition as a function of Al concentration (x) in $Al_xGa_{1-x}As$: solid line (present result), dashed line (Ref. 8). The experimental points (□) are taken from Ref. 8.

alloy disordering by as much as 20 percent in comparison to our calculation. Also shown in Fig. 5 are some experimental values of the σ[9] which are higher than our calculated values. Because the observed linewidth includes effects due to other broadening

mechanisms such as due to random electric fields of residual ionized impurities and clustering in the alloy, which are not included in this model, the experimental linewidths are considerably higher than the calculated values.

B.2.2.3. Alloy Broadening in $Al_xGa_{1-x}As$ and $In_{0.48}Ga_{0.52}P$ Systems

- **Magnetic Field Effect**

In Fig. 6, we show the calculated linewidth associated with an excitonic transition, σ, in $Al_xGa_{1-x}As$ as a function of applied magnetic field strength for a few Al compositions using the present method (solid curves) and those of Mena et al. (dashed curves)[10]. The values of σ obtained in both calculations increase with the applied magnetic field as the exciton is squeezed by the applied field. When B_z is larger than 10 kG, the linewidth for a fixed composition is directly proportional to B_z. Mena and coworkers[10] have predicted a similar result using the classical approach . The values of

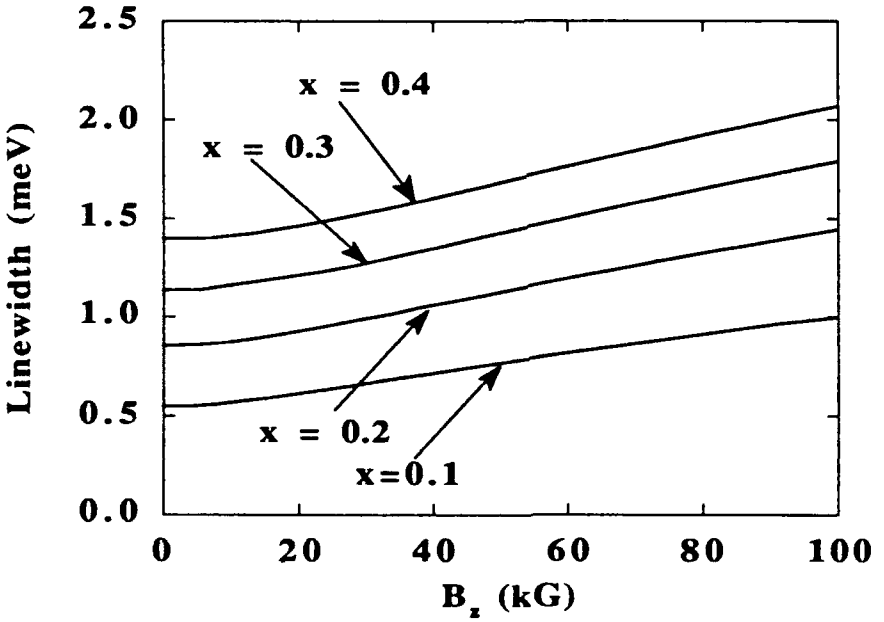

Fig. 6 Variation of the full-width at half-maximum (σ) of the excitonic transition as a function of applied magnetic field strength (B_z) at a few values of Al concentration (x) in $Al_xGa_{1-x}As$.

the linewidths calculated in Ref. 8, however, increase with the applied magnetic field at a considerably faster rate. This is probably due their use of spherical exciton volume for the magneto-exciton that does not have a spherical symmetry.

Recently Eric Jones [11] of Sandia Laboratories has measured the variation of the excitonic linewidth in $In_{0.48}Ga_{0.52}P$ as a function of the magnetic field using photoluminescence spectroscopy. He finds that the value of the linewidth increases by about 1.4 meV when the magnetic field is increased from zero to 135 kG. We have calculated the variation of σ in $In_{0.48}Ga_{0.52}P$ for the above range of the magnetic field and find that it agrees very well with the experimental values.

We are now in the process of extending our formalism to calculate the excitonic linewidths in quantum well structures in the presence of electric and magnetic fields.

B.3. Summary

SUMMARY

We have developed a simple but highly efficient, accurate and versatile method for calculating the exciton binding energies, transition energies, oscillator strengths and absorption coefficients in quantum wells with arbitrary potential profiles in the presence of electric and magnetic fields applied along the growth direction. We have also applied this method to study the energy levels of hydrogenic impurities in wells of arbitrary potential profiles in the presence of electric and magnetic fields. We have developed a quantum mechanical formalism for calculating excitonic linewidths due to compositional disorder in semiconductor alloys which eliminates completely the use of exciton volume. We have extended the this formalism to include the effects of magnetic field.

REFERENCES

1 J. T. Ebner and J. R. Arthur, J. Vac. Sci. Technol. A **5**, 2007 (1987).

2 S. M. Lee and K. K. Bajaj, Phys. Rev. B (in press).

3 S. M. Lee and K. K. Bajaj, to be published.

4 G. D. Sanders and K. K.Bajaj, J. Appl. Phys. **68**, 5348 (1990).

5 G. E. Bauer and T. Ando, Phys. Rev. B **38**, 6015 (1988).
6 R. L. Greene and K. K. Bajaj, Phys. Rev. B **31**, 6498 (1985).
7 J. Cen and K. K. Bajaj, to be published.
8 S. M. Lee and K. K. Bajaj, to be published.
9 J. Singh, K. K Bajaj, Appl. Phys. Lett. **48**, 1077 (1986).
10 R. A. Mena, "*Magnetic field effect on the exciton photoluminescence linewidth of semiconductor alloys*", M. S. Thesis, Arizona State University,1990, unpublished. R. A. Mena, G. D. Sanders, K. K. Bajaj and S. C. Dudley, J. Appl. Phys. **70**, 1866 (1991).
11 Eric Jones (private communication)

C. Publications in technical journals.

R Droopad, R A Puechner, K Y Choi, K T Shiralagi and G N Maracas, "Molecular Beam Epitaxial Growth and Optical Properties of Strained Rectangular and Asymmetric Triangular InGaAs Quantum Well Structures," J. Crystal Growth. **114** (1991) 327.

R.A. Puechner, D.S. Gerber, R. Droopad, and G.N. Maracas, "Nonlinear Electroabsorption in Asymmetric Triangular Quantum Well Self Electro-Optic Effect Devices," Internat. J. Nonlinear Optical Phys., Vol. 1, No. 3, July (1992) (invited paper).

K. T. Shiralagi, R. A. Puechner, K. Y. Choi, R. Droopad, and G. N. Maracas, "Narrow Photoluminescence Linewidth of Quantum Wells Grown by Gas Source Molecular Beam Epitaxy, J. Cryst. Growth,**114** (1991) 337.

R. Droopad, K. Y. Choi, R. A. Puechner, K. T. Shiralagi, D. S. Gerber, G. N. Maracas, "Optical Properties of Strained Asymmetric Triangular InGaAs/GaAs Multiple Quantum Wells," Applied Physics Letters, **59** (1991) 2308..

R. Droopad, R. A. Puechner, K. T. Shiralagi, K. Y. Choi, G. N. Maracas, "Optical Properties of a Single Strained InGaAs/GaAs Quantum Well on Vicinal GaAs Surfaces," Appl. Phys. Lett., **58** (1991) 1777.

R.A. Puechner, D.S. Gerber, D.A. Johnson, R. Droopad and G.N. Maracas," Optical Properties of Asymmetric Triangular Quantum Wells for Self Electro-optic Effect Devices" International Conf. on Nonlinear Optics, Hawaii, 1990.

P. W. Yu, D. C. Reynolds, G. D. Sanders, K. K. Bajaj, C. E. Stutz and K. R. Evans, "Electric Field Effect of Excitons in Asymmetric Triangular AlGaAs/GaAs Quantum Wells." Phys. Rev. B **43**, 4344 (1991).

S. M. Lee and K. K. Bajaj, "Simple Method For Calculating Excitonic Properties in Quantum-Confined Semiconductor Structures with Arbitrary Potential Profiles in the Presence of Applied Fields." Phys. Rev. B (in press).

S. M. Lee and K. K. Bajaj, "A New Theory of Linewidths of Radiative Transitions due to Disordering in Semiconductor Alloys." Appl. Phys. Lett. (in press).

S. M. Lee and K. K. Bajaj, "A Simple Method For Calculating the Excitonic Properties of Semiconductor Quantum Wells of Arbitrary Shapes in the Presence of Both Electric and Magnetic Fields." Submitted for publication in Phys. Rev. B.

J. Cen, S. M. Lee and K. K. Bajaj, "Effect of Electric and Magnetic Fields on Confined Donor States in a Coupled Double Quantum Well." Submitted for publication in Phys. Rev. B.

S. M. Lee, K. K. Bajaj, and E. Jones, "Magnetic Field Dependent Excitonic Photoluminescence Linewidth in Semiconductor Alloys." To be submitted for publication in Phys. Rev. B.

D. Professional personnel associated with the research effort

At Arizona State University
G. N. Maracas, PI
D. L. Mathine, Faculty Associate
R. Droopad, Assistant Research Scientist
K. Choi, Assistant Research Scientist
D. Gerber, Graduate Student
R. Puechner, Graduate Student

At Emory University
K. K. Bajaj, principle investigator.
S. M. Lee, post-doctoral fellow.
J. Cen, post-doctoral fellow.

E. Interactions:

Telephone conversations with AFOSR staff have been on a regular basis to discuss technical and contractual issues and developments. The URI review visit was April 26, 1991 at ASU. View graphs of recent experimental progress were sent in November.

E.1. Papers presented at meetings, conferences, seminars, etc.

K. K. Bajaj, "Quantum Well Based Spatial Light Modulators: Effects of Potential Profile On Their Performance." Presented at the Workshop on Optical Properties of Mesoscopic Semiconductor Structures, April 1991, Snowbird, Utah.

E.2. Consultative and advisory functions to other laboratories and agencies

F. New discoveries, inventions, or patent disclosures and specific applications stemming from the research effort.

G. Other statements.